# PRODUCTION OF $\nu_\tau$ AND $\bar{\nu}_\tau$ IN FIXED TARGET SHiP EXPERIMENT*

Rafał Maciuła

Institute of Nuclear Physics Polish Academy of Sciences
Radzikowskiego 152, 31-342 Kraków, Poland

*(Received May 7, 2020)*

We discuss production cross sections of $\nu_\tau$ and $\bar{\nu}_\tau$ coming from the direct $D_s^\pm \to \tau^\pm \nu_\tau/\bar{\nu}_\tau$ and chain $D_s^\pm \to \tau^+/\tau^- \to \bar{\nu}_\tau/\nu_\tau$ decays in $p$+$^{96}$Mo scattering with proton beam $E_{\rm lab} = 400$ GeV *i.e.* at $\sqrt{s}_{NN} = 27.4$ GeV. We include two different $D_s^\pm$ meson production mechanisms: via charm fragmentation $c \to D_s^+$ and $\bar{c} \to D_s^-$ as well as via subleading fragmentation of strange quarks/antiquarks $s \to D_s^-$ and $\bar{s} \to D_s^+$. Estimates of a number of observed $\nu_\tau/\bar{\nu}_\tau$ in the $\nu_\tau/\bar{\nu}_\tau$ +$^{208}$Pb reaction, with 2 m long target are given.

DOI:10.5506/APhysPolB.51.1461

## 1. Introduction

The $\nu_\tau$ and $\bar{\nu}_\tau$ particles were the ones of last ingredients of the Standard Model discovered experimentally [1]. So far, only a few $\nu_\tau$ neutrinos and $\bar{\nu}_\tau$ antineutrinos were observed experimentally in the DONuT [2], OPERA [3] and IceCube [4] detectors. The proposed SHiP (Search for Hidden Particles) experiment [5, 6] may change the situation [7]. It was roughly estimated that about 300–1000 neutrinos ($\nu_\tau + \bar{\nu}_\tau$) will be observed by the SHiP experiment [7, 8]. This will considerably improve our knowledge in this weakly tested corner of the Standard Model.

The $\nu_\tau/\bar{\nu}_\tau$ neutrinos/antineutrinos are known to be primarily produced from $D_s^\pm$ decays. The corresponding branching fraction is relatively well-known [9] and is BR($D_s^\pm \to \tau^\pm \nu_\tau/\bar{\nu}_\tau$) = 0.0548. The $D_s$ mesons are copiously produced in proton–proton collisions at the LHC. They were measured *e.g.* by the ALICE [10] and LHCb experiments [11] at $\sqrt{s} = 7$ TeV. The LHCb experiment in the collider-mode has observed even a small asymmetry in the production of $D_s^+$ and $D_s^-$ [12]. So far, the asymmetry is not

* Presented at XXVI Cracow Epiphany Conference on LHC Physics: Standard Model and Beyond, Kraków, Poland, January 7–10, 2020.

fully understood from first principles. Recently, its possible explanation in terms of subleading $s \to D_s^-$ or $\bar{s} \to D_s^+$ fragmentations was proposed [13]. However, the corresponding light-to-heavy fragmentation functions are not well-known.

Here, we wish to investigate in detail forward production of $D_s$ mesons and forward production of $\nu_\tau$ neutrinos and $\bar{\nu}_\tau$ antineutrinos. In the proposed model, $D_s^\pm$ mesons can be produced from both, charm and strange quark/antiquark fragmentation, with a similar probability of the transition (8% and 3% respectively). The $s \to D_s$ mechanism is expected to be especially important at large rapidities (or large Feynman $x_{\rm F}$) [13]. In the present paper, we wish to analyze whether this fact has consequences for forward production of neutrinos/antineutrinos in the SHiP experiment or not. The main goal is to make as realistic as possible predictions of the cross section for production of $\nu_\tau/\bar{\nu}_\tau$ neutrinos/antineutrinos. To make the studies complete, interactions of the neutrinos/antineutrinos with the matter in the case of the Pb target will be also discussed.

## 2. $D_s^\pm$ meson production

In the present paper, we discuss two mechanisms of $D_s$ meson production:

— $c \to D_s^+$, $\bar{c} \to D_s^-$, called leading fragmentation,

— $\bar{s} \to D_s^+$, $s \to D_s^-$, called subleading fragmentation.

The underlying leading-order pQCD partonic mechanisms for charm and strange quark production are shown schematically in Fig. 1 and Fig. 2, respectively. At high energies, for charm-quark production higher-order (NLO and even NNLO) corrections are very important, especially when considering differential distributions, such as quark transverse momentum distribution or squark–antiquark correlation observables (see *e.g.* Refs. [14, 15]). The $c$ and $\bar{c}$ cross sections are calculated in the collinear NLO approximation using the FONLL framework [16].

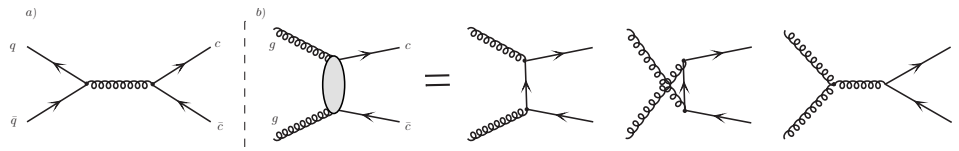


Fig. 1. Dominant mechanisms of charm-quark production at leading order: $q\bar{q}$-annihilation (diagram (a)) and $gg$-fusion (diagrams (b)). These partonic processes lead to leading (standard) fragmentation component of $D_s$ production.

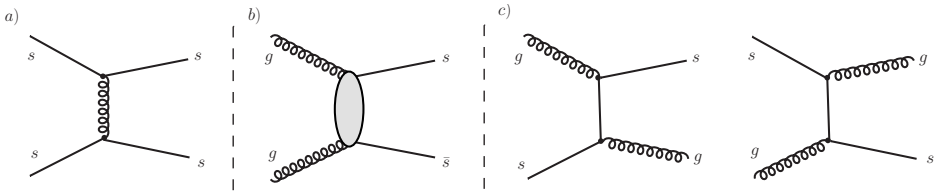


Fig. 2. An example of strange quark (or antiquark) production mechanisms at leading order: $ss \to ss$ (diagram (a)), $gg \to s\bar{s}$ (diagram (b)), $gs \to gs$ and $sg \to sg$ (diagrams (c)). These partonic processes lead to subleading (unfavored) fragmentation component of $D_s$ production.

Not all charm hadrons must be created from the $c/\bar{c}$ fragmentation. An extra hidden associated production of $c$ and $\bar{c}$ can occur in a complicated hadronization process. In principle, $c$ and $\bar{c}$ partons can also hadronize into light mesons (*e.g.* kaons) with non-negligible fragmentation fraction (see *e.g.* Ref. [17]). Similarly, fragmentation of light partons into heavy mesons may be equally possible [18]. In the present study, we will also discuss results of our simple model of subleading fragmentation $s \to D_s^-$ and $\bar{s} \to D_s^+$ [13].

The $s$ and $\bar{s}$ distributions are calculated here in the leading-order (LO) collinear factorization approach with on-shell initial-state partons and with a special treatment of minijets at low transverse momenta, as adopted *e.g.* in PYTHIA, by multiplying standard cross section by a somewhat arbitrary suppression factor [19]

$$F_{\rm sup}(p_{\rm t}) = \frac{p_{\rm t}^4}{\left(\left(p_{\rm t}^0\right)^2 + p_{\rm t}^2\right)^2}\,. \tag{1}$$

Within this framework, the cross section, of course, strongly depends on the free parameter $p_{\rm t}^0$ which could be, in principle, fitted to low-energy charm experimental data [20]. Here, we use rather conservative value $p_{\rm t}^0 = 1.5$ GeV. We use two different sets of the collinear parton distribution functions (PDFs): the MMHT2014 [21] and the NNPDF30 [22] parametrizations. Both of them provide an asymmetric strange sea quark distributions in the proton with $s(x) \neq \bar{s}(x)$. The dominant partonic mechanisms are $gs \to gs$, $g\bar{s} \to g\bar{s}$ (and their symmetric counterparts) and $gg \to s\bar{s}$.

The transition from quarks to hadrons in our calculations is done within the independent parton fragmentation picture. Here, we follow the assumptions relevant for the case of low c.m.s. collision energies and/or small transverse momenta of hadrons, as discussed in our recent analysis [23], and we assume that the hadron $H$ is emitted in the direction of parent quark/antiquark $q$, *i.e.* $\eta_H = \eta_q$ (the same pseudorapidities or polar angles). Within this approach, we set the light-cone $z$-scaling, *i.e.* we define $p_H^+ = z p_q^+$, where $p^+ = E + p$. For $c/\bar{c} \to D_s^\pm$ fragmentation, we take the tra-

ditional Peterson fragmentation function with $\varepsilon = 0.05$ (see Fig. 3). In contrast to the standard mechanism, the fragmentation function for $s/\bar{s} \to D_s^{\mp}$ transition is completely unknown which makes the situation more difficult. For the case of light-to-light (light parton to light meson) transition, rather soft fragmentation functions (peaked at small $z$-values) are supported by phenomenological studies [24]. The massless gluon fragmentation to heavy open charm meson is also possible (see *e.g.* Ref. [18]). On the other hand, in the case of $B_c$ meson production, the $b \to B_c$ fragmentation function was found to be peaked at large-$z$, while the function for $c \to B_c$ transition is shifted to intermediate $z$-values [25]. In principle, one could expect a similar behaviour of the $c \to D_s$ and $s \to D_s$ fragmentation functions. Therefore, as a default set in the following calculations, we take for the $s/\bar{s} \to D_s^{\mp}$ transition the Peterson fragmentation function with $\varepsilon = 0.5$ which is peaked at intermediate $z$-values (see Fig. 3).

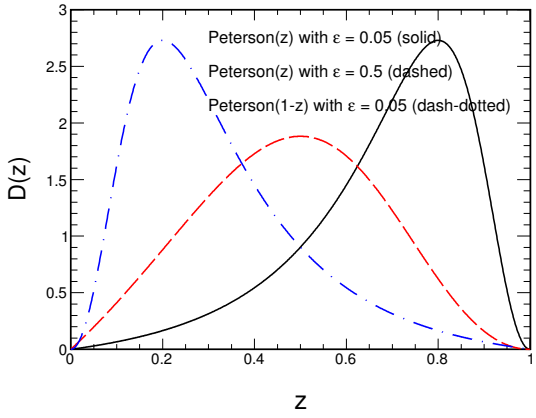


Fig. 3. The Peterson fragmentation function for $\varepsilon = 0.05$ (solid) and $\varepsilon = 0.5$ (dashed) as well as the reversed Peterson function for $\varepsilon = 0.05$ (dash-dotted).

Besides the shape of the $s/\bar{s} \to D_s^{\mp}$ fragmentation function, the relevant fragmentation fraction is also unknown. The transition probability $P = P_{s \to D_s}$ can be treated as a free parameter and needs to be extracted from experimental data. First attempt was done very recently in Ref. [13], where $D_s^+/D_s^-$ production asymmetry was studied. To make the following predictions more precise, we repeat our calculations of the $D_s^+/D_s^-$ production asymmetry from Ref. [13] but for more up-to-date PDF sets and for different fragmentation functions (shown in Fig. 3). The updated predictions for the asymmetry are presented in Fig. 4.

In Fig. 5, we show the resulting energy distribution of $D_s$ mesons in the laboratory frame from proton–proton scattering at $\sqrt{s} = 27.4$ GeV. We compare contributions of the leading ($c/\bar{c} \to D_s^{\pm}$) and the subleading ($s/\bar{s} \to D_s^{\mp}$) mechanisms, calculated in the FONLL and in the LO collinear

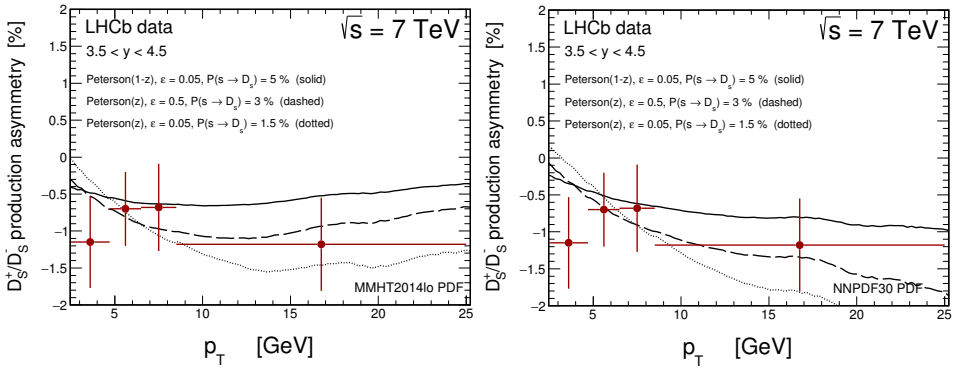


Fig. 4. The $D_s^+/D_s^-$ production asymmetry obtained with our approach from Ref. [13] for $\sqrt{s} = 7$ TeV at forward rapidities together with the LHCb experimental data [12]. The left panel corresponds to the MMHT2014 PDFs and the right panel corresponds to the NNPDF30 PDF.

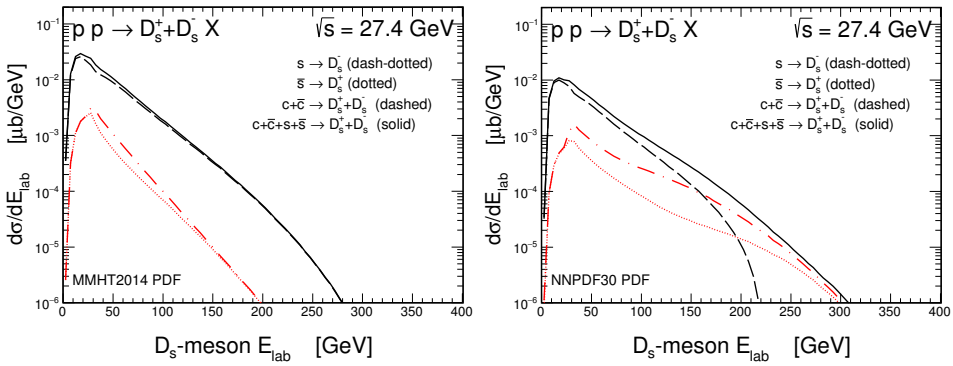


Fig. 5. Energy distributions of $D_s$ mesons in the laboratory frame for the MMHT2014 (left) and the NNPDF30 (right) sets of collinear PDFs. Contributions from charm and strange quark fragmentation are shown separately. Details are specified in the figure.

approach, respectively. In this calculation, $P_{c\to D_s} = 0.08$ and $P_{s\to D_s} = 0.03$ were used. Here, we show separately the leading $c + \bar{c} \to D_s^+ + D_s^-$ (dashed lines) and two subleading $s \to D_s^-$ (dash-dotted lines) and $s \to D_s^-$ (dotted lines) contributions as well as their sum $c + \bar{c} + s + \bar{s} \to D_s^+ + D_s^-$ (solid lines). The left and right panels correspond to the MMHT2014 and the NNPDF30 PDFs, respectively. A pretty much different results are obtained for the two different PDF sets, especially for large meson energies. Depending on the collinear PDFs used, our model leads to a rather small (the MMHT2014 PDF) or a fairly significant (the NNPDF30 PDF) contribution to the $D_s$ meson production at large energies which comes from the $s/\bar{s}$-quark fragmentation.

Summarizing this part, we see big uncertainties in our predictions for the production of $D_s$ mesons at the low $\sqrt{s} = 27.4$ GeV energy. A future measurement of $D_s$ mesons at low energies would definitely help to better understand underlying mechanism and, in consequence, improve predictions for $\nu_\tau/\bar{\nu}_\tau$ production for the SHiP experiment.

## 3. Direct decay of $D_s^\pm$ mesons

The considered here decay channels: $D_s^+ \to \tau^+\nu_\tau$ and $D_s^- \to \tau^-\bar{\nu}_\tau$, which are the sources of the direct neutrinos, are analogous to the standard text book cases of $\pi^+ \to \mu^+\nu_\mu$ and $\pi^- \to \mu^-\bar{\nu}_\mu$ decays, discussed in detail in the past (see *e.g.* Ref. [26]). The same formalism used for the pion decay applies also to the $D_s$ meson decays. Since pion has spin zero, it decays isotropically in its rest frame. However, the produced muons are polarized in its direction of motion which is due to the structure of weak interaction in the Standard Model. The same is true for $D_s^\pm$ decays and polarization of $\tau^\pm$ leptons.

Therefore, the $\tau$ decay must be carefully considered. In such decays, the $\tau$ particles are strongly polarized with $P_{\tau^+} = -P_{\tau^-}$. In the following, we assume that in the rest frame of $D_s$ meson

$$P_{\tau^-} = 1 \quad \text{and} \quad P_{\tau^+} = -1\,.$$

This is also very good approximation in the rest frame of $\tau^\pm$.

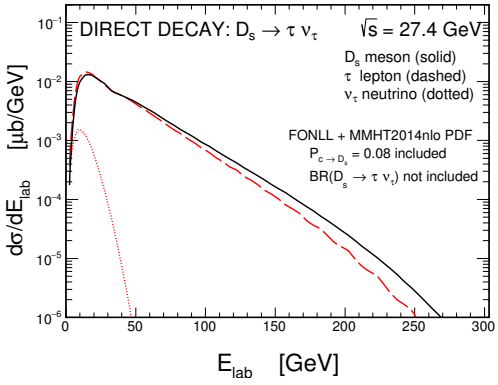


Fig. 6. Laboratory energy distributions of $D_s$ mesons (solid), $\tau$ leptons (dashed) and $\nu_\tau$ neutrinos (dotted) from the direct decay $D_s^\pm \to \tau^\pm\nu_\tau/\bar{\nu}_\tau$. Here, we show only the leading contribution to $D_s$ meson production in proton–proton collisions from charm quarks calculated with the FONLL code. The decay branching fraction is not included here for easier comparison.

To calculate cross section for $\nu_\tau/\bar{\nu}_\tau$ production, the $D_s^\pm \to \tau^\pm \nu_\tau/\bar{\nu}_\tau$ branching fraction must be included. The decay branching fraction is rather well-known: $\mathrm{BR}(D_s^\pm \to \tau^\pm \nu_\tau/\bar{\nu}_\tau) = 0.0548 \pm 0.0023$ [9].

In Fig. 6, we show laboratory frame energy distribution of $D_s$ meson (solid line), $\tau$ lepton (dashed line) and $\nu_\tau$ neutrino (dotted line) from the direct decay. Here, the presented cross sections are for proton–proton interactions. It can be clearly seen that the $\tau$ lepton takes almost the whole energy of the mother $D_s$ meson.

## 4. Neutrinos from chain decay of $\tau$ leptons

The $\tau$ decays are rather complicated due to having many possible decay channels [9]. Nevertheless, all confirmed decays lead to production of $\nu_\tau$ ($\bar{\nu}_\tau$). This means that the total amount of neutrinos/antineutrinos produced from $D_s$ decays into $\tau$ lepton is equal to the amount of antineutrinos/neutrinos produced in subsequent $\tau$ decay. However, their energy distributions will be different due to $D_s$ production asymmetry in the case of the subleading fragmentation mechanism.

The purely leptonic channels (three-body decays), analogous to the $\mu^\pm \to e^\pm(\bar{\nu}_\mu/\nu_\mu)(\nu_e/\bar{\nu}_e)$ decay (discussed *e.g.* in Refs. [26, 28]) cover only about 35% of all $\tau$ lepton decays. Remaining 65% are semi-leptonic decays. They differ quite drastically from each other and each gives slightly different energy distribution for $\nu_\tau$ ($\bar{\nu}_\tau$). In our model for the decay of $D_s$ mesons, there is almost full polarization of $\tau$ particles with respect to the direction of their motion.

Since $P_{\tau^+} = -P_{\tau^-}$ (see the previous subsection) and the angular distributions of polarized $\tau^\pm$ are antisymmetric with respect to the spin axis, the resulting distributions of $\nu_\tau$ and $\bar{\nu}_\tau$ from decays of $D_s^\pm$ are then identical, consistent with CP symmetry (see *e.g.* Ref. [27]).

The mass of the $\tau$ lepton (1.777 GeV) is very similar to the mass of the $D_s$ meson (1.968 GeV). Therefore, the direct neutrino takes away only a small fraction of energy/momentum of the mother $D_s$. In this approximation,

$$\vec{v}_\tau = \vec{v}_{D_s}\,, \qquad \vec{p}_\tau = \vec{p}_{D_s} \tag{2}$$

polarization of $\tau$ in its rest frame is 100%. In reality, polarization of $\tau^\pm$ is somewhat smaller. In the approximate $Z$-moment method often used for production of neutrinos/antineutrinos in the atmosphere discussed *e.g.* in Ref. [28], the polarization is a function of $E_\tau/E_{D_s}$ (see also Ref. [29]).

Before we go to distribution of neutrinos/antineutrinos in the laboratory system (fixed target $p + {}^{96}\mathrm{Mo}$ collisions), we shall present distributions of neutrinos/antineutrinos in the $\tau^\pm$ center-of-mass system, separately for different decay channels of $\tau$. In this calculation, we use TAUOLA code [30].

## 5. Neutrino/antineutrino interactions with the Pb target

How many neutrinos/antineutrinos will be observed in the SHiP experiment depends on the cross section for neutrino/antineutrino scattering of nuclei off the target. In the case of the SHiP experiment, a dedicated lead target was proposed. At not too small energies ($\sqrt{s_{NN}} > 5$ GeV), the cross section for $\nu_\tau$Pb and $\bar{\nu}_\tau$Pb interactions can be obtained from elementary cross sections as

$$\sigma(\nu_\tau \mathrm{Pb}) = Z\sigma(\nu_\tau p) + (A - Z)\sigma(\nu_\tau n)\,, \tag{3}$$

$$\sigma(\bar{\nu}_\tau \mathrm{Pb}) = Z\sigma(\bar{\nu}_\tau p) + (A - Z)\sigma(\bar{\nu}_\tau n)\,. \tag{4}$$

Shadowing effects depend on $x$ variable (parton longitudinal momentum fraction), *i.e.* on neutrino/antineutrino energy. At not too high energies (not too small $x$), shadowing effects are rather small and can be neglected at present accuracy having in mind other uncertainties. On the other hand, for the $x$-ranges considered here, the antishadowing and/or EMC-effect may appear non-negligible but still rather small and shall not affect the numerical predictions presented here. The nuclear modifications of the PDFs goes beyond the scope of the present study and will be considered elsewhere.

The probability of interacting of neutrino/antineutrino with the lead target can be calculated as

$$P^{\mathrm{target}}_{\nu_\tau/\bar{\nu}_\tau}(E) = \int_0^d n_{\mathrm{cen}} \sigma_{\nu_\tau \mathrm{Pb}}(E) \mathrm{d}z = n_{\mathrm{cen}} \sigma_{\nu_\tau \mathrm{Pb}}(E) d\,, \tag{5}$$

where $n_{\mathrm{cen}}$ is a number of scattering centers (lead nuclei) per volume element and the target thickness is $d \approx 2$ m [7]. Using the NuWro Monte Carlo generator [31], we obtain $\sigma(E)/E \sim 1.09 \times 10^{-38}$ cm$^2$/GeV for neutrino and $0.41 \times 10^{-38}$ cm$^2$/GeV for antineutrino for the $E = 100$ GeV. The number of scattering centers is

$$n_{\mathrm{cen}} = (11.340/207.2) N_{\mathrm{A}}\,, \tag{6}$$

where $N_{\mathrm{A}} = 6.02 \times 10^{23}$ is the Avogadro number.

The energy dependent flux of neutrinos can be written as

$$\Phi_{\nu_\tau/\bar{\nu}_\tau}(E) = \frac{N_p}{\sigma_{pA}} \mathrm{d}\sigma_{pA \to \nu_\tau}(E)/\mathrm{d}E\,, \tag{7}$$

where $N_p$ is integrated number of beam protons ($N_p = 2 \times 10^{20}$ according to the current SHiP project). The $\sigma_{pA}$ in Eq. (7) is a crucial quantity which requires a short discussion. Usually, it is defined as $\sigma_{pA} = A\,\sigma_{pN}$, where

$\sigma_{pN}$ is the inelastic hadronic cross section per nucleon on a target with $A$ nucleons. For the molybdenum target, the latter is rather not well-known. In Refs. [5, 8], it was taken to be equal to $\sigma_{pN} = 10.7$ mb which is obtained from the approximate expression $\sigma_{pN} = \sigma_{pA}/A = 1/\lambda_{\rm int}\rho N_{\rm A}$, where $\lambda_{\rm int}$ is the nuclear interaction length, $\rho$ is the target density and $N_{\rm A}$ is the Avogadro number. A realistic estimation of the quantity at this stage is not simple and the number is rather uncertain.

The formula from Eq. (7) can be used to estimate number of neutrinos/antineutrinos produced at the beam dump. For the decays of $D_s$ meson produced from charm quark fragmentation, it reads

$$N_{\nu_\tau} = 2\frac{N_p}{\sigma_{pA}}\sigma_{pA\to\nu_\tau X} = 2\frac{N_p}{\sigma_{pN}}\sigma_{pp\to c\bar{c}X}\ {\rm BR}(D_s^\pm \to \tau^\pm\nu_\tau/\bar{\nu}_\tau)\ {\rm P}(c\to D_s)\,. \tag{8}$$

The factor of 2 accounts for neutrinos from the direct decay of $D_s^+$ and neutrinos from the chain decay of $D_s^-$. A similar formula can be written for antineutrinos. Taking ${\rm P}(c\to D_s) = 0.08$, ${\rm BR}(D_s^\pm \to \tau^\pm\nu_\tau/\bar{\nu}_\tau) = 0.0548$, $\sigma_{pp\to c\bar{c}X} = 10\ \mu$b, and $\sigma_{pN} = 20$ mb, we get $N_{\nu_\tau} = 1.32\times 10^{15}$. The number $\sigma_{pN} = 20$ mb is a bit larger than the corresponding numbers used in Refs. [5, 6, 8] and leads to rather more conservative predictions for $N_{\nu_\tau}$. This appears to account for the small (about factor 2) discrepancy with the corresponding results for $N_{\nu_\tau}$ presented there, *i.e.* $2.85\times 10^{15}$ in Ref. [5] and $3.1\times 10^{15}$ in Ref. [6]. Summarizing, the number of neutrinos is rather uncertain mostly due to the choice of $\sigma_{pA}$ and $pp\to c\bar{c}X$ cross sections. In general, for the $pA$ inelastic cross section, one could expect slightly different scaling with $A$ as for $pA$ production of charm pairs in Eq. (8).

Finally, the number of neutrinos/antineutrinos observed in the Pb target is calculated from the formula

$$N^{\rm target}_{\nu_\tau/\bar{\nu}_\tau} = \int {\rm d}E\Phi_{\nu_\tau/\bar{\nu}_\tau}(E)P^{\rm target}_{\nu_\tau/\bar{\nu}_\tau}(E)\,. \tag{9}$$

Here, $\Phi_{\nu_\tau/\bar{\nu}_\tau}(E)$ is calculated from different approaches to $D_s$ meson production including their subsequent decays and $P^{\rm target}_{\nu_\tau/\bar{\nu}_\tau}(E)$ is obtained using Eq. (5). The cross sections for neutrino/antineutrino interactions with the lead target is shown in Fig. 7 and are calculated using the NuWro Monte Carlo generator.

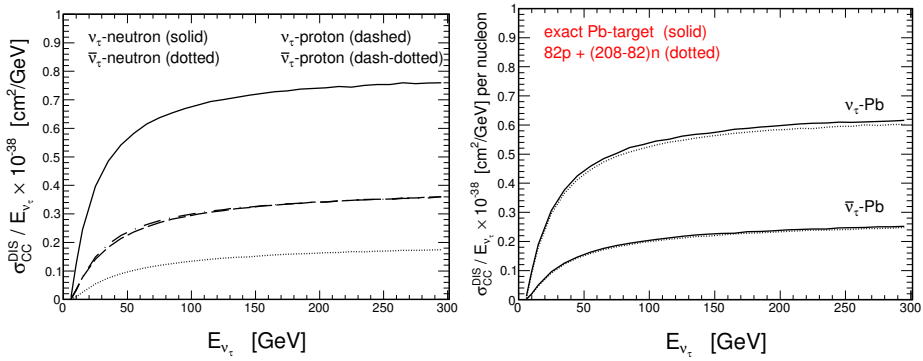


Fig. 7. Left: The elementary cross sections $\sigma(\nu_\tau p)$, $\sigma(\nu_\tau n)$, $\sigma(\bar{\nu}_\tau p)$ and $\sigma(\bar{\nu}_\tau n)$ as a function of neutrino/antineutrino energy. Right: The $\sigma(\nu_\tau \mathrm{Pb})$ and $\sigma(\bar{\nu}_\tau \mathrm{Pb})$ cross sections per nucleon as a function of neutrino/antineutrino energy. The results are obtained within the NuWro Monte Carlo generator. Details are specified in the figure.

## 6. Numerical predictions for the SHiP experiment

After integrating the integrands of the integral in Eq. (9), one gets numbers of neutrinos/antineutrinos collected in Table I. Quite different numbers are obtained for the different considered scenarios. We get larger numbers than in Ref. [8] but smaller than in Ref. [7]. The chain contribution is significantly larger (by about factor of 7) than the direct one. For the MMHT2014 distribution, the contribution of the leading mechanism is much larger than for the subleading one (by about factor of 10). For the NNPDF30 distributions, the situation is changed and the difference between the leading and the subleading components is much smaller (by about factor of 2). We pre-

TABLE I

Number of observed $\nu_\tau$ and $\bar{\nu}_\tau$ for the SHiP experiment.

| Framework/mechanism | Number of observed neutrinos | | | | |
|---|---|---|---|---|---|
| | Flavour | Direct | Chain | $\nu_\tau + \bar{\nu}_\tau$ | $\frac{\nu_\tau - \bar{\nu}_\tau}{\nu_\tau + \bar{\nu}_\tau}$ |
| FONLL + NNPDF30 NLO<br>$c/\bar{c} \to D_s^\pm \to \nu_\tau/\bar{\nu}_\tau$ | $\nu_\tau$<br>$\bar{\nu}_\tau$ | 96<br>27 | 515<br>180 | 818 | 0.49 |
| LO coll. + NNPDF30 LO<br>$s/\bar{s} \to D_s^\pm \to \nu_\tau/\bar{\nu}_\tau$ | $\nu_\tau$<br>$\bar{\nu}_\tau$ | 28<br>22 | 336<br>49 | 435 | 0.67 |
| FONLL + MMHT2014nlo<br>$c/\bar{c} \to D_s^\pm \to \nu_\tau/\bar{\nu}_\tau$ | $\nu_\tau$<br>$\bar{\nu}_\tau$ | 277<br>80 | 1427<br>508 | 2292 | 0.49 |
| LO coll. + MMHT2014lo<br>$s/\bar{s} \to D_s^\pm \to \nu_\tau/\bar{\nu}_\tau$ | $\nu_\tau$<br>$\bar{\nu}_\tau$ | 17<br>7 | 142<br>37 | 203 | 0.58 |

dict large observation asymmetry (see the last column) for $\nu_\tau$ and $\bar{\nu}_\tau$. This asymmetry is bigger than shown *e.g.* in Refs. [7, 8]. This is due to the subleading mechanism for $D_s^\pm$ meson production included in the present paper. The observation asymmetry for the leading contribution which comes from the differences of the $\nu_\tau$ and $\bar{\nu}_\tau$ interactions with target is estimated at the level of 50%. In the case of the subleading contribution, the asymmetry increases to 60–70%, depending on PDF model.

## 7. Conclusions

In the present paper, we have discussed the mechanism and cross sections for production of $\nu_\tau$ and $\bar{\nu}_\tau$ in fixed target experiment for $\sqrt{s_{NN}} = 27.4$ GeV with 400 GeV proton beam and molybdenum target. In the present analysis, we have assumed that the neutrinos/antineutrinos are produced exclusively from $D_s^\pm$ mesons. Other, probably small, contributions (Drell–Yan, $\gamma\gamma$ fusion, $B$ decays, *etc.*) have been neglected here.

We include two different contributions of $D_s$ meson production: the leading fragmentation of $c$ and $\bar{c}$ and the subleading fragmentation of $s$ and $\bar{s}$. The subleading fragmentation leads to asymmetry provided $s$ and $\bar{s}$ distributions are different. We have discussed a possible role of the subleading production of $D_s$ mesons in the context of "increasing" the production of $\nu_\tau/\bar{\nu}_\tau$ neutrino/antineutrino at the SHiP experiment. A similar effect for production of high-energy $\nu_\tau/\bar{\nu}_\tau$ neutrinos/antineutrinos was discussed very recently in Ref. [13]. The subleading fragmentation may increase the probability of observing $\nu_\tau/\bar{\nu}_\tau$ neutrinos/antineutrinos by the planned SHiP fixed target experiment at CERN. We have found that present knowledge of $s/\bar{s}$ parton distributions and especially $s/\bar{s}$ fragmentation to $D_s$ mesons does not allow for precise estimations. The SHiP experiment could be therefore useful to test $s/\bar{s}$ distributions.

More details of the present study can be found in the original publication [33].

## REFERENCES

[1] DONuT Collaboration (K. Kodama *et al.*), *Phys. Lett. B* **504**, 218 (2001).
[2] DONuT Collaboration (K. Kodama *et al.*), *Phys. Rev. D* **78**, 052002 (2008).
[3] OPERA Collaboration (N. Agafonova *et al.*), *Phys. Rev. Lett.* **120**, 211801 (2018); *Erratum ibid.* **121**, 139901 (2018).
[4] IceCube Collaboration, private communications.
[5] SHiP Collaboration (M. Anelli *et al.*), arXiv:1504.04956 [physics.ins-det].
[6] S. Alekhin *et al.*, *Rep. Prog. Phys.* **79**, 124201 (2016).

[7] SHiP Collaboration (A. Buonaura), *PoS* **DIS2016**, 260 (2016), arXiv:1609.04860 [physics.ins-det].
[8] W. Bai, M.H. Reno, *J. High Energy Phys.* **1902**, 077 (2019).
[9] Particle Data Group (M. Tanabashi *et al.*), *Phys. Rev. D* **98**, 030001 (2018).
[10] ALICE Collaboration (B. Abelev *et al.*), *Phys. Lett. B* **718**, 279 (2012).
[11] LHCb Collaboration (R. Aaij *et al.*), *Nucl. Phys. B* **871**, 1 (2013).
[12] LHCb Collaboration (R. Aaij *et al.*), *J. High Energy Phys.* **1808**, 008 (2018).
[13] V.P. Goncalves, R. Maciuła, A. Szczurek, *Phys. Lett. B* **794**, 29 (2019).
[14] M. Cacciari *et al.*, *J. High Energy Phys.* **1210**, 137 (2012), arXiv:1205.6344 [hep-ph].
[15] R. Maciuła, A. Szczurek, *Phys. Rev. D* **100**, 054001 (2019).
[16] M. Cacciari, M. Greco, P. Nason, *J. High Energy Phys.* **1998**, 007 (1998); M. Cacciari, S. Frixione, P. Nason, *J. High Energy Phys.* **2001**, 006 (2001).
[17] M. Epele, C. García Canal, R. Sassot, *Phys. Lett. B* **790**, 102 (2019).
[18] T. Kneesch, B.A. Kniehl, G. Kramer, I. Schienbein, *Nucl. Phys. B* **799**, 34 (2008).
[19] T. Sjöstrand *et al.*, *Comput. Phys. Commun.* **191**, 159 (2015).
[20] R. Maciuł, A. Szczurek, *Phys. Rev. D* **97**, 074001 (2018).
[21] L.A. Harland-Lang, A.D. Martin, P. Motylinski, R.S. Thorne, *Eur. Phys. J. C* **75**, 204 (2015).
[22] NNPDF Collaboration (R.D. Ball *et al.*), *J. High Energy Phys.* **1504**, 040 (2015).
[23] R. Maciuła, A. Szczurek, *J. Phys. G: Nucl. Part. Phys.* **47**, 035001 (2020), arXiv:1907.13388 [hep-ph].
[24] NNPDF Collaboration (V. Bertone *et al.*), *Eur. Phys. J. C* **77**, 516 (2017).
[25] X.C. Zheng, C.H. Chang, T.F. Feng, X.G. Wu, *Phys. Rev. D* **100**, 034004 (2019).
[26] P. Renton, «Electroweak Interactions: An Introduction to the Physics of Quarks and Leptons», *Cambridge University Press*, 1990, p. 596.
[27] S.M. Barr, T.K. Gaisser, P. Lipari, S. Tilav, *Phys. Lett. B* **214**, 147 (1988).
[28] T.K. Gaisser, «Cosmic Rays and Particle Physics», *Cambridge University Press*, Cambridge, UK 1990, p. 279.
[29] L. Pasquali, M.H. Reno, *Phys. Rev. D* **59**, 093003 (1999).
[30] S. Jadach, J.H. Kuhn, Z. Wąs, *Comput. Phys. Commun.* **64**, 275 (1991); M. Jeżabek, Z. Wąs, S. Jadach, J.H. Kuhn, *Comput. Phys. Commun.* **70**, 69 (1992); S. Jadach, Z. Wąs, R. Decker, J.H. Kuhn, *Comput. Phys. Commun.* **76**, 361 (1993); M. Chrzaszcz, T. Przedzinski, Z. Was, J. Zaremba, *Comput. Phys. Commun.* **232**, 220 (2018).
[31] J. Żmuda, K.M. Graczyk, C. Juszczak, J.T. Sobczyk, *Acta Phys. Pol. B* **46**, 2329 (2015).
[32] SHiP Collaboration (H. Dijkstra, T. Ruf), «Heavy Flavour Cascade Production in a Beam Dump», CERN-SHiP-NOTE-2015-009.
[33] R. Maciuła, A. Szczurek, J. Zaremba, I. Babiarz, *J. High Energy Phys.* **2001**, 116 (2020).